

# INVESTIGATING THE CONNECTION BETWEEN QUASI PERIODIC OSCILLATIONS AND SPECTRAL COMPONENTS WITH NuSTAR DATA OF GRS 1915+105

ANJALI RAO JASSAL, SANTOSH V. VADAWALE, AND MITHUN N. P. S  
 Physical Research Laboratory, Ahmedabad- 380009, India

RANJEEV MISRA

Inter-University Center for Astronomy and Astrophysics, Post Bag 4, Ganeshkhind, Pune 411007, India  
 Draft version August 8, 2018

## ABSTRACT

The low frequency quasi periodic oscillations (QPOs) are commonly observed during hard states of black hole binaries. Several studies have established various observational/empirical correlations between spectral parameters and QPO properties, indicating a close link between the two. However, the exact mechanism of generation of QPO is not yet well understood. In this paper, we present our attempts to comprehend the connection between the spectral components and the low frequency QPO observed in GRS 1915+105 using the data from NuSTAR. Detailed spectral modeling as well as the presence of the low frequency QPO and its energy dependence during this observation have been reported by Miller et al. (2013) and Zhang et al. (2015) respectively. We investigate the compatibility of the spectral model and energy dependence of the QPO by simulating light curves in various energy bands for small variation of the spectral parameters. The basic concept here is to establish connection, if any, between the QPO and the variation of either a spectral component or a specific parameter, which in turn can shed some light on the origin of the QPO. We begin with the best fit spectral model of Miller et al. (2013) and simulate the light curve by varying the spectral parameter at frequencies close to the observed QPO frequency in order to generate the simulated QPO. Further we simulate similar light curves in various energy bands in order to reproduce the observed energy dependence of RMS amplitude of the QPO. We find that the observed trend of increasing RMS amplitude with energy can be reproduced qualitatively if the spectral index is assumed to be varying with the phases of the QPO. Variation of any other spectral parameter does not reproduce the observed energy dependence.

*Subject headings:* accretion, accretion disks — black hole physics — X-rays: binaries — X-rays: individual (GRS 1915+105)

## 1. INTRODUCTION

Accreting black hole binaries show variability on a wide range of timescales from milli-seconds to months and years. While the long term variability typically arises due to the transient nature or the state transitions, the short term (sub-second) variability is generally attributed to the processes in the inner regions of accretion disk. A perplexing feature of such a short term variability is the presence of quasi periodic oscillations, characterized by a narrow peak superimposed over a broad band noise in the power density spectrum (PDS). QPOs have been observed in a frequency range of less than Hz to hundreds of Hz (Remillard & McClintock 2006) and they are generally classified as low frequency QPOs (LFQPOs, 0.1-30 Hz) and high frequency QPOs (HFQPOs, 40-450 Hz). Frequency of HFQPOs does not vary with a sizeable change in luminosity suggesting that it depends on the fundamental system parameters such as black hole mass and spin (Remillard & McClintock 2006; Remillard et al. 2006).

It is evident that the LFQPOs are not linked with the orbital motion of the material in the disk because the observed frequencies correspond to the far outer regions of the accretion disk. The properties of these QPOs (e.g. low frequency break, centroid frequency, rms amplitude) are strongly coupled with the changes in spectrum and luminosity (see Munro et al. 1999; Sobczak et al. 2000;

Vignarca et al. 2003; Li et al. 2014), suggesting that these QPOs originate in the same inner region of the accretion disk. Despite the knowledge of empirical correlations of QPO properties with spectral parameters (e.g. Sobczak et al. 2000; Stiele et al. 2013), the exact physics is not very well understood. There are several models to explain the origin and properties of LFQPOs. In one of the most promising models, the LFQPO originates as a result of relativistic Lense-Thirring (LT) precession of the hot inner flow (Stella & Vietri 1998; Wagoner et al. 2001; Schnittman et al. 2006; Ingram & Done 2012). The model successfully explains the variation of frequencies of QPO centroid and the low frequency break in terms of variation in the truncation radius of the inner disk. Another model based on the accretion ejection instability suggests that a QPO is produced by a spiral pattern rotating at a frequency of a few tenths of the Keplerian frequency at the inner edge of the disk (Tagger & Pellat 1999; Varnière et al. 2002; Rodriguez et al. 2002). However, according to the shock oscillation model, wherein a shock is formed by a centrifugal barrier in a region of lower viscosity, LFQPOs are originated due to oscillation of the post-shock region (Molteni et al. 1996; Chakrabarti et al. 2004; Garain et al. 2014).

Most of the available QPO models explain the frequencies and some of the observed correlations along with other timing and spectral properties. However, in many

cases, the models are silent about the energy dependence of the QPO or the exact mechanism of origin of the QPO. Observing a QPO as a direct oscillation of one or more spectral parameter could provide much deeper insights in the modulation mechanism and thus origin of the QPO. In this context, here we attempt to investigate the observed energy dependence of the LFQPO in GRS 1915+105 in terms of modulation of the spectral parameters.

GRS 1915+105 is one of the most enigmatic black hole binary system famous for its relativistic jets exhibiting superluminal motion (Mirabel & Rodríguez 1994) and a variety of variability patterns (Fender & Belloni 2004). Its LFQPOs and their correlations with various other parameters have been studied extensively (Maccarone et al. 2011; Mikles et al. 2006; Rodríguez et al. 2002; Munro et al. 1999; Morgan et al. 1997, etc.). However, another intriguing aspect of this system is the spin of the black hole. Various reports have found spin of GRS 1915+105 ranging from 0.56 (Blum et al. 2009) to  $\sim 0.98$  (McClintock et al. 2006; Blum et al. 2009). Probably, the most accurate spin estimate for GRS 1915+105 is available from the NuSTAR observation (Miller et al. 2013, hereafter M13), where the lower values of spin are ruled out at a high level of confidence based on the accurate modeling of relativistically blurred reflection. This observation belongs to a special state of GRS 1915+105 known as ‘plateau’ state and it shows a QPO with frequency of 1.5 Hz. Properties of this LFQPO have been studied in detail by Zhang et al. (2015, hereafter Z15) where the authors show that the RMS amplitude of the QPO increases with energy with a characteristic flattening between 10–20 keV. This suggests the possibility of an interplay between independently varying spectral parameters. Thus investigation of the spectral parameter(s), which lead to the observed energy dependence of the QPO power can provide significant clues on the origin of the QPO.

In this context, here we delve into the energy dependence of the QPO power by means of simulating light curves by varying different spectral parameter(s). In the next section, we discuss the NuSTAR observation and its analysis to reproduce the results of M13 and Z15. The results of these spectral and timing analysis are used to generate the simulated light curve as explained in the following section, with the discussion on our findings and preliminary conclusions in the subsequent sections.

## 2. OBSERVATION AND DATA ANALYSIS

The NuSTAR observation of GRS 1915+105 carried out on July 03, 2012 has been used for the present study. The same observation has been analyzed in detail by M13 and Z15 for spectroscopic and timing studies respectively. We extract the spectrum following M13 and adopt their best fit model, `tbabs*(kerrconv*reflionx_hc + cutoffpl)` where the reflection of the primary cut-off power law is modeled by `reflionx_hc` (a variant of `reflionx` model), which assumes the incident spectrum as cut-off power law. With the same spectral model, we ensure that the best fit results are almost identical, which are then used in our simulations as explained in the next section.

We also carried out the timing analysis on the line of Z15. The light curves are extracted in an energy range of 3–80 keV with a bin size of 100 ms. PDS is generated for each interval of 1024 bins and co-added for all the intervals. The PDS from both FPMA and FPMB show a very strong type-C QPO at  $\sim 1.5$  Hz. The PDS also shows strong spikes at every 1 Hz, however, it is known that these are instrumental artifacts in the early NuSTAR observations and hence we ignore these bins during fitting in XSPEC. The light curves from FPMA and FPMB are added together in order to improve the statistics and the PDS is generated from the combined light curve (Fig. 1 left panel). We fit the PDS using multiple lorentzians and a constant, which takes care of white noise level in the PDS. It is obvious that the PDS has many complex features such as broad band noise, a small peak at frequency of  $\sim 0.75$  Hz and a strong QPO at  $\sim 1.5$  Hz. Here we concentrate only on the  $\sim 1.5$  Hz QPO feature because it is known to have systematic dependence on energy (Fig. 1 right panel). The small peak at  $\sim 0.75$  Hz has been described as a sub-harmonic by Z15. However for the purpose of the present work, we consider it as a part of broad band noise mainly because of very low Q value of  $\sim 3.6$ . Z15 have reported that the RMS amplitude of the QPO increases with energy. We verify this from the light curves in different energy bands (3–4 keV, 4–5 keV, 5–6 keV, 6–7 keV, 7–9 keV, 9–12 keV, 12–15 keV and 15–30 keV).

We find an increasing trend with a shallow dip (or flattening) in 10–20 keV as reported in Z15 (Fig. 1 right panel). They have also reported that this observation shows increase in count rate as well as QPO frequency during the later part (after  $\sim 40$  ks of the start of the observation). Therefore, we restrict both the spectral and timing analysis to the first 40 ks of data, where the count rate and QPO frequency are quite stable. Effective exposure times for our analysis are 9.71 ks and 10.01 ks for FPMA and FPMB respectively.

## 3. LIGHT CURVE SIMULATION AND RESULTS

In many cases, the observed spectrum can be explained with different models with same statistical significance. In such cases, the compatibility of a spectral model with the observed timing characteristic can be helpful to solve the degeneracy. The main objective of the present work is to investigate the compatibility of the observed QPO properties with the spectral model. One possibility to achieve this is by comparing the amplitude of the oscillations across multiple energy bands. Another possibility is by comparing the phase lags in a similar manner. Black hole binaries are known for showing phase lags between different energy bands. Phase lags for GRS 1915+105 has also been reported by several authors (e.g Reig et al. 2000; Qu et al. 2010; Lin et al. 2000), wherein it is generally found that the hard photons lag the soft photons. We also calculated phase lags between different energy bands using NuSTAR data, however because of the relatively poor statistics (compared to e.g. RXTE-PCA), the phase lags can not be constrained (obtained values are consistent with zero with larger error bars) with the present data. Hence we adopt the alternate method by comparing the observed energy dependence of the QPO RMS amplitude with the simulated energy dependence.

An important feature of the present best fit spectral

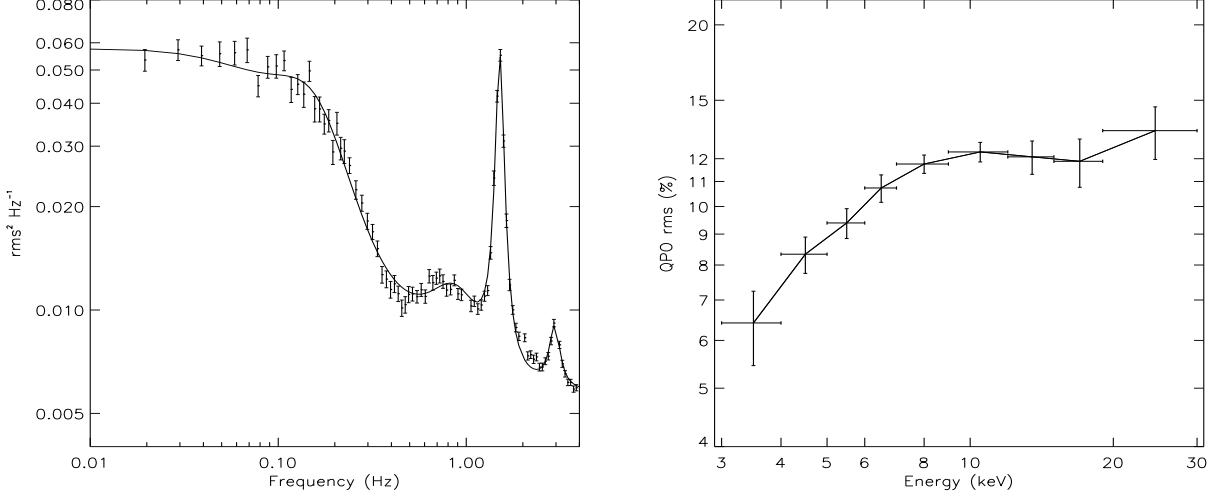


**Figure 1.** Figure shows the observed PDS (left) in the energy range of 3-80 keV and the energy dependence of QPO power (right).

**Table 1**

The best fit spectral parameters calculated with the model `tbabs*(kerrconv@reflionx_hc + cutoffpl)`. Errors indicate 90% confidence intervals.

Parameter	Best fit value
$N_H$ ( $\times 10^{22} \text{cm}^{-2}$ )	$4.43^{+0.18}_{-0.05}$
Index 1	$9.99_{-0.06}$
Index 2	$0.01^{+0.02}$
$R_{in}$ ( $R_g$ )	$7.49^{+0.07}_{-0.06}$
$a_*$	$0.973^{+0.002}_{-0.002}$
$i$	$65.41^{+1.02}_{-0.39}$
$\Gamma$	$1.709^{+0.001}_{-0.001}$
$X_i$	$993.0^{+14.8}_{-19.0}$
$A_{Fe}$	$0.97^{+0.02}_{-0.13}$
Cut-off Energy	$35.47^{+1.19}_{-0.18}$
$N_{ref}$ ( $\times 10^{-5}$ )	$1.19^{+0.20}_{-0.02}$
$N_{pl}$	$1.907^{+0.008}_{-0.007}$

model is that it consists of only one primary continuum component, cut-off power law, covering the full energy range. Hence, it does not allow interpretation of the QPO in terms of oscillation of one of the spectral component as suggested by Rao et al. (2000) (also corroborated by Vadawale et al. 2001, 2003). Thus observed energy dependence of the QPO power must result from the variation of one or more spectral parameters.

Here we assume that a particular spectral parameter varies with a frequency close to the observed QPO frequency. We consider four possible parameters of the spectral model, viz. the spectral index, normalization of the cut-off power law, normalization of the reflection component and the ionization parameter; which can vary with the phases of the QPO. Though the high energy cut-off can vary, we keep it fixed at the best fit value because its variation does not affect the model in the energy range of interest. All parameters of `kerrconv` are assumed not to vary with the phases of the QPO. We then simulate the light curve with a bin size of 100 ms. Initially we simulate the light curve for variation of only one parameter. As a zeroth order approximation, we assume that the parameter is varying sinusoidally with QPO phases in a range centered at the best fit value. The assumption of sinusoidal oscillation is clearly an over simplification

and the actual oscillation profile could be more complex. However, the energy dependence of RMS amplitude is not likely to have strong dependence on the exact shape of oscillations. We also include a small random variation over the sinusoidal variation to be a bit more realistic. Later we also simulate the light curve for multiple parameters varying simultaneously. In either case the basic algorithm for simulation of light curve is as follows-

It is assumed that a parameter  $\alpha$  obtained from the best-fit spectral model varies at a frequency close to the observed QPO frequency ( $\bar{\nu}$ ). The amplitudes of the sinusoidal variation and random fluctuation are  $p_\alpha$  and  $q_\alpha$  respectively such that  $q_\alpha = r p_\alpha$ . The simulation is carried out for  $r=0.1, 0.2$  and  $0.3$  and it is found that the results remain unaffected. Therefore, we present results hereafter for  $r=0.1$  (i.e. 10% random variations superimposed over the sinusoidal oscillations).

- Let  $m_\alpha$  be the best fit value of parameter  $\alpha$ .
- The spectral model is evaluated in `XSPEC` with the parameter  $\alpha$  assuming values in the range  $m_\alpha \pm p_\alpha$ , keeping the rest of the parameters at their best fit values. Model counts, including the effects of detector response matrix as well as effective area,

are obtained in each of the energy bins and are tabulated.

- The light curve is simulated with a bin size of 100 ms for a duration of  $\sim 10$  ks to match the exposure time of the observation.
- For each interval ( $\sim 2$  s) a random frequency of oscillation ( $\nu$ ) is drawn from a lorentzian distribution with the mean  $\bar{\nu}$  ( $=1.5$  Hz) and the FWHM ( $=0.089$  Hz) values same as those for the observed QPO. The frequency remains the same throughout an interval. We have also verified that the overall results remain unaffected if the frequency is changed more often within one interval. It is assumed here that the quasi periodic nature arises due to frequency modulation (see Rao et al. 2010).
- The phase of oscillation for each time bin  $i$  is obtained by

$$\phi_i = 2 \pi \nu \Delta t + \phi_{i-1}$$

where  $\Delta t$  is the bin size and  $\phi_{i-1}$  is the phase for previous time bin. Continuity of the phases across intervals is also maintained in the same manner.

- The value assumed by parameter  $\alpha$  for the  $i$ -th timebin is calculated as

$$\alpha_i = p_\alpha \sin(\phi_i) + q_\alpha z_i$$

where  $z_i$  is a standard normal variate (see Fig 5, left panel).

- Mean counts in the time bin  $i$  for a given energy bin  $j$  ( $C_{ji}$ ) corresponding to value  $\alpha_i$  is obtained from the table generated in the first step. The energy bin  $j$  is kept same as that used to extract the observed light curves.
- Random number is generated from Poisson distribution with mean  $C_{ji}$  and is recorded as counts in the  $i$ -th time bin of the light curve in energy bin  $j$ .
- Power density spectra are generated for these simulated light curves using POWSPEC and are fitted with XSPEC as usual.

Fig (2) shows a section of the simulated light curve and its PDS in an energy range of 9–12 keV. It should be noted that we have not included low frequency noise in our simulations because our primary objective here is to investigate the energy dependence of the QPO power. Fig (3) summarizes the overall results of our simulations. The four panels show the simulated energy dependence of the QPO power for variation of the four spectral parameters. The observed energy dependence is shown with black solid line in all the panels. For each parameter, multiple lines are shown corresponding to the three different range of variation of parameters. It can be seen that only the variation of spectral index can reproduce the overall trend of the increasing QPO power with energy. Variation of other three parameters cannot reproduce the observed trend. Even in the case of the spectral index variation, the exact shape of the energy dependence curve, particularly the dip or flattening in the energy range of 10–20 keV is not reproduced. This suggests

that, while the variation of spectral index during QPO phases is essential it is not the only source of the variability. Hence we test the hypothesis by simulating the light curves considering the variation of more than one parameter simultaneously. The simulation was repeated for the variation of two and three parameters and the results are shown in Fig (4) and (5) respectively. Since the reflection component represents the Comptonization component reflected from the disk, it is expected that the former would be stronger for a harder spectrum. Or in other words, the reflection component should be anti-correlated with the spectral index. Therefore, the parameters of reflection component ( $N_{ref}$  and  $Xi$ ) were varied out of phase with spectral index in the simulation of light curves. Panel A of Fig (4) shows the energy dependence obtained from the variation of reflection normalization ( $N_{ref}$ ) and spectral index and Panel B shows the results for ionization parameter ( $Xi$ ) and spectral index. A comparison of Panel A of Fig (3) and Fig (4) shows that the variation of spectral index and normalization of reflection reproduce the observed energy dependence more closely than the variation of spectral index alone. We also studied the energy dependence with the light curves simulated by varying 1) normalization of cut-off power law and normalization of reflection component and 2) normalization of cut-off power law and ionization parameter. The variation of the two set of parameters does not reproduce the observed increasing trend of QPO power.

We have further attempted to reproduce the observed pattern by varying three parameters simultaneously. The left panel of Fig (5) shows the variation of spectral parameters with time. Representative results obtained from the variation of three parameters are shown in the right panel of Fig (5). It can be seen that the results start resembling the observed pattern more closely. We avoid attempts to exactly reproduce the observed pattern as this will require detailed fine tuning of the specifics such as number of varying parameters, amplitudes of variation, phase lags etc. More importantly, a relook into the spectral model itself might also be necessary which is beyond the scope of this paper. The main objective here is to convey that the present best fit spectral model is compatible with the observed trend of the increasing QPO power with energy when the spectral index is assumed to be varying. However, it might be necessary to look beyond this model in order to reproduce the exact energy dependence of the QPO power.

#### 4. DISCUSSION AND CONCLUSIONS

Increasing trend of the LFQPO power with energy is well known (e.g. Tomsick & Kaaret 2001; Rodriguez et al. 2004, 2008). The trend can also be seen in the results shown by Zdziarski et al. (2005); Sobolewska & Życki (2006). However, origin of this trend in terms of variation of the spectral components has not been investigated so far. Here we attempt to explain the energy dependence of LFQPO observed during the first NuSTAR observation of GRS 1915+105. We simulate the light curve for variation of various spectral parameters and compare the resultant energy dependence with the observed one. We find that only variation of the spectral index reproduces the overall trend of the increasing QPO power with energy. Variation of



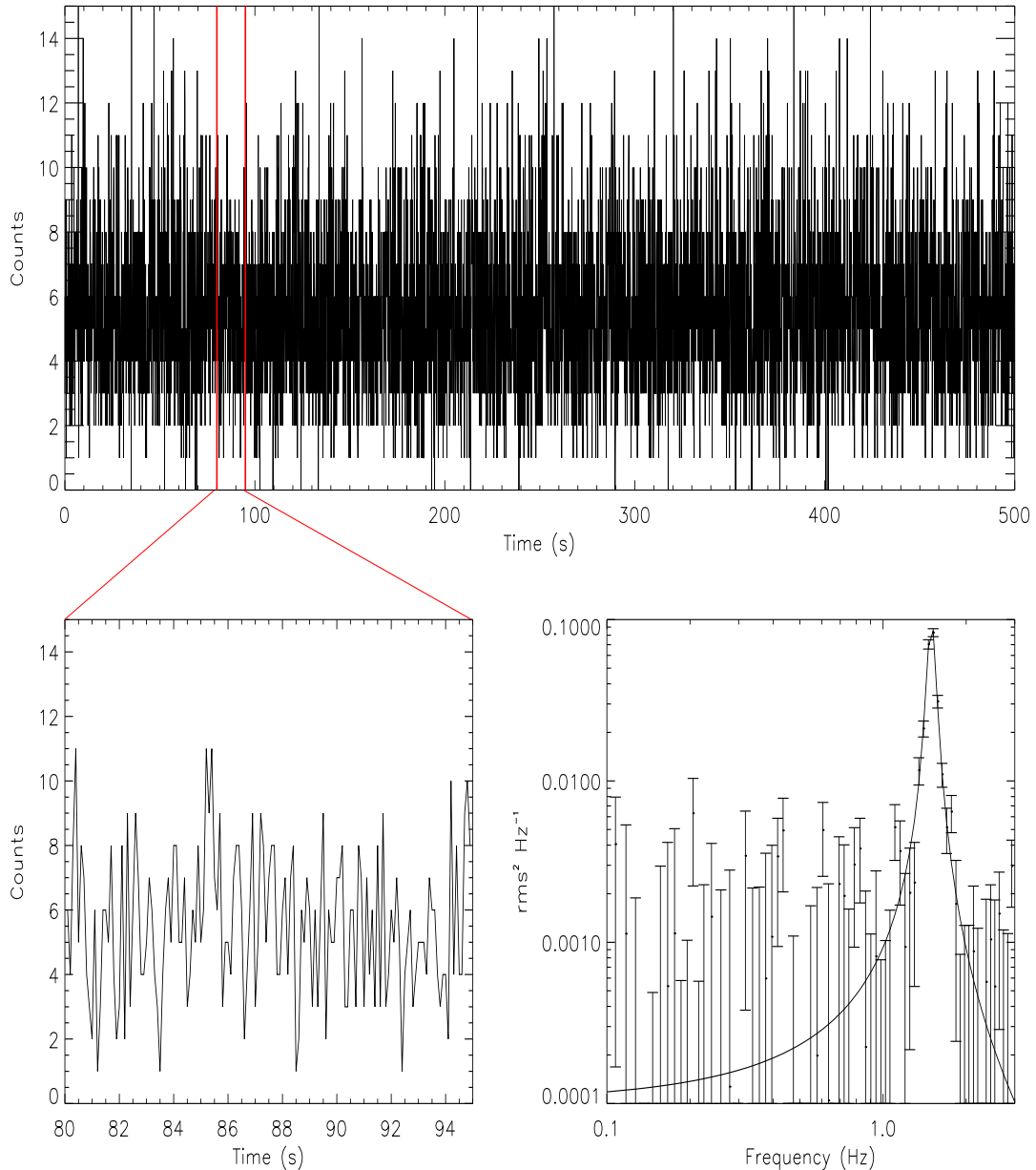


**Figure 2.** The upper panel shows the first 500 seconds of a 9-12 keV light curve simulated by modulating the spectral index. A zoomed-in view of a section of the light curve is shown in the lower-left panel. PDS of the full light curve is shown in lower right panel.

any other parameter does not reproduce the observed trend. This has significant implications on the feasibility of various models proposed to explain the origin of the QPO. For example, the fact that the variation of reflection normalization does not reproduce the observed trend suggests that the QPO models based on geometric modulation (Miller & Homan 2005) may not be realistic.

Among the other existing models for the low frequency QPOs, the model based on Lense-Thirring precession is considered the most successful model. It successfully explains the overall shape of the PDS and the variation of QPO frequency with the changes in spectral hardness, which is further linked with the truncation radius of the inner disk (Ingram & Done 2010). However, the energy dependence of QPO is

not apparently clear. The similar situation exists with a magnetohydrodynamic model for QPO based on the accretion ejection instability (Tagger & Pellat 1999; Varnière et al. 2002; Rodriguez et al. 2002). The shock oscillation model (Molteni et al. 1996; Chakrabarti et al. 2004; Garain et al. 2014) does produce the spectral variation and it could be compatible with the energy dependent QPO power. However, the simulation results obtained from the present spectral model cannot be directly compared with the predictions of shock oscillation model. It might be necessary to perform similar simulation with appropriate model and then verify the results.

Another observation is the flattening of QPO spectrum at 10-20 keV which cannot be reproduced with variation of only spectral index. The flattening seems to be

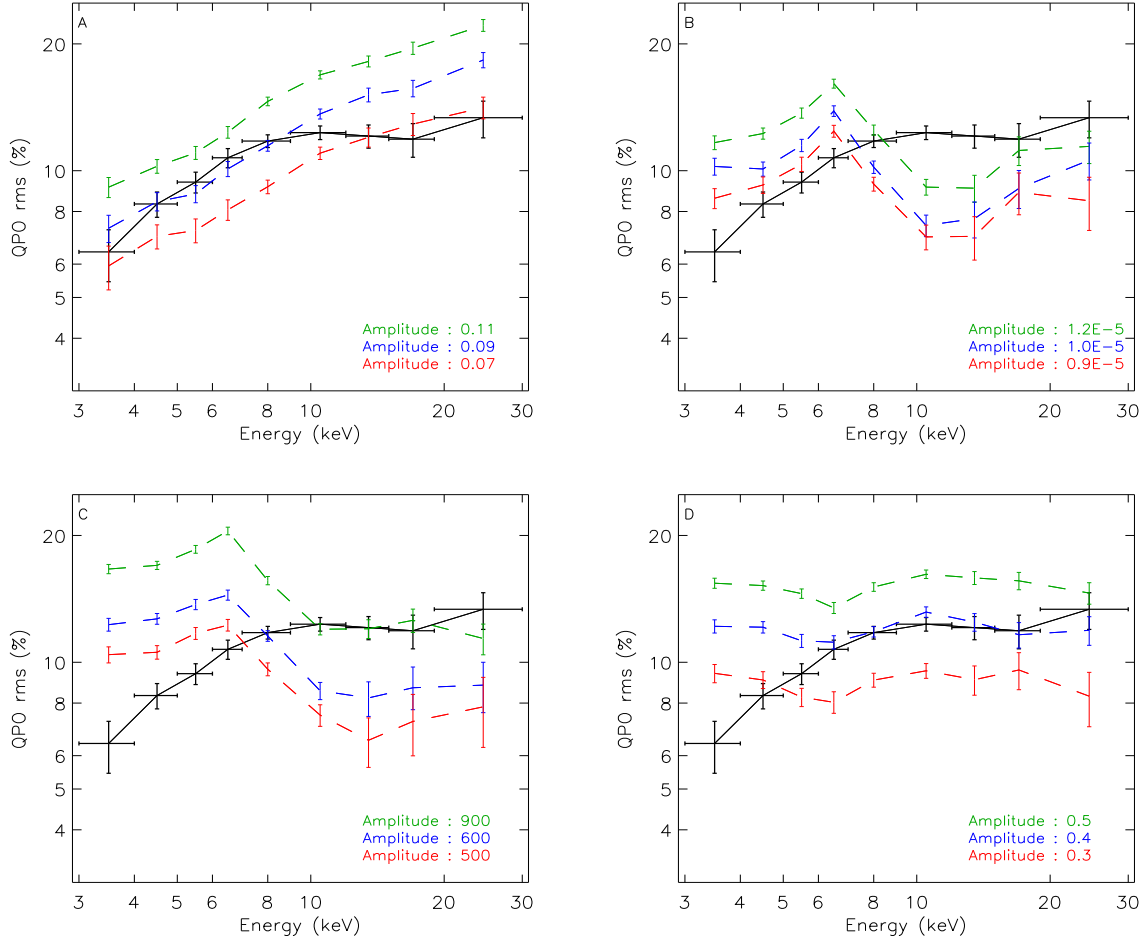


**Figure 3.** Figure shows the simulated energy dependence of QPO obtained by modulation of spectral index (A), normalization of reflionx\_hc (B), ionization parameter (C) and normalization of cut-off power law (D). The dashed lines correspond to simulation results for different amplitudes of modulation. The observed energy dependence is shown with black solid line in all the panels.

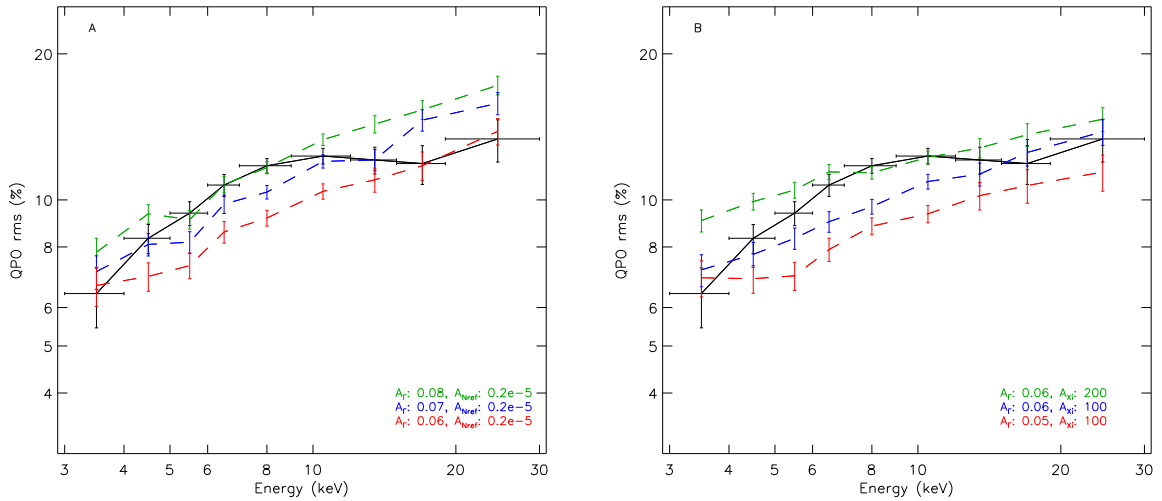


**Figure 4.** Plot showing the energy dependence of QPO with the simulated light curves by varying two parameter simultaneously. Panel A shows the results obtained from the variation of normalization of reflection and spectral index. Panel B shows the result for the variation of ionization parameter and spectral index. The dashed lines correspond to simulation results for different amplitudes of modulation. The observed energy dependence is shown with black solid line in both the panels.

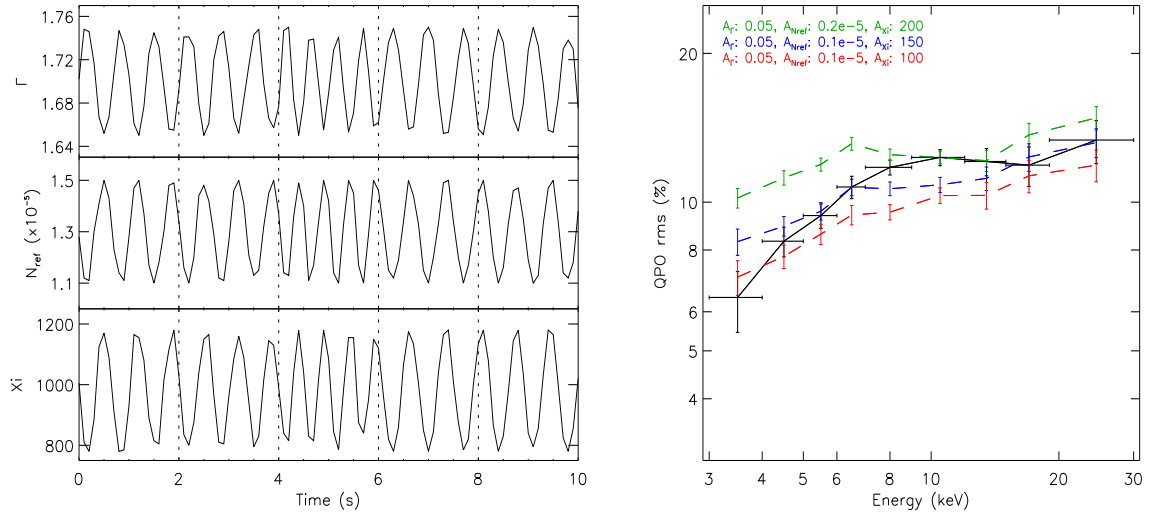


**Figure 5.** The left panel shows the variation of three spectral parameters; spectral index ( $\Gamma$ ), reflionx\_hc normalization ( $N_{ref}$ ), and ionization parameter ( $\xi$ ). The reflection normalization and ionization are varied in same phase which are assumed to be anti-correlated to the phase of spectral index variation. The dashed lines separate the intervals corresponding to different frequencies of modulation. The right panel shows the simulated energy dependence of QPO power obtained by modulation of three parameters. Amplitudes of modulation for  $\Gamma$ ,  $N_{ref}$ , and  $\xi$  are mentioned in the figure.

more common as it has been observed at many other occasions (e.g. Tomsick & Kaaret 2001; Rodriguez et al. 2004, 2008; Zdziarski et al. 2005; Sobolewska & Życki 2006). Similar feature is also found in few other sources (Li et al. 2013). We have verified that the same feature is found in the RXTE observations of GRS 1915+105 during the ‘plateau’ states. We fit the spectra during these observations with the present spectral model consisting of cut-off power law and relativistically blurred reflection. The best fit spectral parameters are similar to that found for the present NuSTAR spectrum. We performed similar simulations using RXTE spectra and could reproduce the overall trend of increasing power of QPO. However, the flattening is not found in the simulation results. The observed flattening might be an indicator of the presence of more than one continuum component as suggested by Rodriguez et al. (2004).

Overall our simulation results can put significant constraints on the modulation mechanism assumed in various present theoretical models of QPO. Recently, Axelsson & Done (2015) have made an attempt to understand QPOs with frequency resolved spectroscopy. We suggest that the QPO phase-resolved spectroscopy, similar to that shown by Ingram & van der Klis (2015) can be another promising way to validate the spectral models, but with full energy resolution spectra. Recently launched Indian astronomy mission Astrosat (Singh et al. 2014), with large effective area of the LAXPC instrument, will provide ample opportunities for such QPO phase-resolved spectroscopy owing to its event mode data over broad energy range.

This research has made use of data obtained from High Energy Astrophysics Science Archive Research Center (HEASARC), provided by NASA’s Goddard Space Flight Center. Research at Physical Research Laboratory is supported by Department of Space, Govt. of India. We thank A. C. Fabian and M. Parker for providing `reflionx_hc` model. We acknowledge the anonymous referee for his/her valuable comments.

## REFERENCES

- Axelsson, M., & Done, C. 2015, ArXiv e-prints  
 Blum, J. L., Miller, J. M., Fabian, A. C., et al. 2009, *ApJ*, 706, 60  
 Chakrabarti, S. K., Acharyya, K., & Molteni, D. 2004, *A&A*, 421, 1  
 Fender, R., & Belloni, T. 2004, *ARA&A*, 42, 317  
 Garain, S. K., Ghosh, H., & Chakrabarti, S. K. 2014, *MNRAS*, 437, 1329  
 Ingram, A., & Done, C. 2010, *MNRAS*, 405, 2447  
 —. 2012, *MNRAS*, 419, 2369  
 Ingram, A., & van der Klis, M. 2015, *MNRAS*, 446, 3516  
 Li, Z. B., Gao, H. Q., Zhang, Z., et al. 2014, *MNRAS*, 440, 143  
 Li, Z. B., Zhang, S., Qu, J. L., et al. 2013, *MNRAS*, 433, 412  
 Lin, D., Smith, I. A., Liang, E. P., & Böttcher, M. 2000, *ApJ*, 543, L141  
 Maccarone, T. J., Uttley, P., van der Klis, M., Wijnands, R. A. D., & Coppi, P. S. 2011, *MNRAS*, 413, 1819  
 McClintock, J. E., Shafee, R., Narayan, R., et al. 2006, *ApJ*, 652, 518  
 Mikles, V. J., Eikenberry, S. S., & Rothstein, D. M. 2006, *ApJ*, 637, 978  
 Miller, J. M., & Homan, J. 2005, *ApJ*, 618, L107  
 Miller, J. M., Parker, M. L., Fuerst, F., et al. 2013, *ApJ*, 775, L45  
 Mirabel, I. F., & Rodríguez, L. F. 1994, *Nature*, 371, 46  
 Molteni, D., Sponholz, H., & Chakrabarti, S. K. 1996, *ApJ*, 457, 805  
 Morgan, E. H., Remillard, R. A., & Greiner, J. 1997, *ApJ*, 482, 993  
 Muno, M. P., Morgan, E. H., & Remillard, R. A. 1999, *ApJ*, 527, 321  
 Qu, J. L., Lu, F. J., Lu, Y., et al. 2010, *ApJ*, 710, 836  
 Rao, A. R., Naik, S., Vadawale, S. V., & Chakrabarti, S. K. 2000, *A&A*, 360, L25  
 Rao, F., Belloni, T., Stella, L., Zhang, S. N., & Li, T. 2010, *ApJ*, 714, 1065  
 Reig, P., Belloni, T., van der Klis, M., et al. 2000, *ApJ*, 541, 883  
 Remillard, R. A., & McClintock, J. E. 2006, *ARA&A*, 44, 49  
 Remillard, R. A., McClintock, J. E., Orosz, J. A., & Levine, A. M. 2006, *ApJ*, 637, 1002  
 Rodriguez, J., Corbel, S., Hannikainen, D. C., et al. 2004, *ApJ*, 615, 416  
 Rodriguez, J., Varnière, P., Tagger, M., & Durouchoux, P. 2002, *A&A*, 387, 487  
 Rodriguez, J., Shaw, S. E., Hannikainen, D. C., et al. 2008, *ApJ*, 675, 1449  
 Schnittman, J. D., Homan, J., & Miller, J. M. 2006, *ApJ*, 642, 420  
 Singh, K. P., Tandon, S. N., Agrawal, P. C., et al. 2014, in *Society of Photo-Optical Instrumentation Engineers (SPIE) Conference Series*, Vol. 9144, Society of Photo-Optical Instrumentation Engineers (SPIE) Conference Series, 1  
 Sobczak, G. J., McClintock, J. E., Remillard, R. A., et al. 2000, *ApJ*, 531, 537  
 Sobolewska, M. A., & Życki, P. T. 2006, *MNRAS*, 370, 405  
 Stella, L., & Vietri, M. 1998, *ApJ*, 492, L59  
 Stiele, H., Belloni, T. M., Kalemci, E., & Motta, S. 2013, *MNRAS*, 429, 2655  
 Tagger, M., & Pellat, R. 1999, *A&A*, 349, 1003  
 Tomsick, J. A., & Kaaret, P. 2001, *ApJ*, 548, 401  
 Vadawale, S. V., Rao, A. R., Naik, S., et al. 2003, *ApJ*, 597, 1023  
 Vadawale, S. V., Rao, A. R., Nandi, A., & Chakrabarti, S. K. 2001, *A&A*, 370, L17  
 Varnière, P., Rodriguez, J., & Tagger, M. 2002, *A&A*, 387, 497  
 Vignarca, F., Migliari, S., Belloni, T., Psaltis, D., & van der Klis, M. 2003, *A&A*, 397, 729  
 Wagoner, R. V., Silbergleit, A. S., & Ortega-Rodríguez, M. 2001, *ApJ*, 559, L25  
 Zdziarski, A. A., Gierliński, M., Rao, A. R., Vadawale, S. V., & Mikołajewska, J. 2005, *MNRAS*, 360, 825  
 Zhang, L., Chen, L., Qu, J.-l., & Bu, Q.-c. 2015, *AJ*, 149, 82